

Visual Stimuli Generated by Biochemical Reactions Discrete Chaotic Dynamics as a Basis for Neurofeedback

Olga Grechko, MSc
Vladimir Gontar, PhD

ABSTRACT. *Introduction.* In this article a novel methodology for a neurofeedback system is proposed. It is based on the visual stimuli generated by the distributed biochemical reactions discrete chaotic dynamics (BRDCD) of brain neurons. These visual stimuli take the form of symmetrical colored images known as mandalas.

Method. The proposed biofeedback system applies a BRDCD mathematical model to transform an on-line recording of EEG signals into a simulated time-series EEG and into computer generated series of mandala images. Thus, these images represent experimentally measured EEG and therefore reflect the subject's mental state.

Results. It will be shown that good qualitative similarity between simulated and experimental EEG was achieved. The examples of generating series of mandala images using experimental EEG will be demonstrated.

Conclusion. Based on Jung's theory of the healing power of the psychological phenomenon of mandala images, it is proposed that visual stimuli in the form of mandalas could facilitate fast and effective neurofeedback training, thereby providing a therapeutic effect.

KEYWORDS. Discrete chaotic dynamics, EEG, mandala symbolism, neurofeedback

INTRODUCTION

It is well known that visual stimuli and/or feedback play an important role in neurofeedback training processes (Thompson & Thompson, 2003). In this work, we present an innovative method for creating visual stimuli for use in neurofeedback. The proposed visual stimuli take the form of symmetrical colored images known as mandalas. According to Jung (1973), the majority of

mandalas are circular images containing patterns in multiples of four in the form of a cross, a star, a square, and so on, although individual mandalas may present a variety of different motifs and patterns. Jung found that, as a psychological phenomenon, mandalas appear spontaneously in dreams, in certain states of conflict, and in cases of schizophrenia. He considered the mandala images painted by his patients to reflect their mental state in attempts at self-healing. In

Olga Grechko is affiliated with Ben-Gurion University of the Negev, Negev, Israel.

Vladimir Gontar is affiliated with Ben-Gurion University of the Negev, Negev, Israel.

Address correspondence to: Olga Grechko, MSc, Department of Industrial Engineering and Management, Ben-Gurion University of the Negev, Negev, Israel (E-mail: grachko@bgu.ac.il).

The authors acknowledge, with thanks, the financial support of the Israel Ministry of Science.

his book *Mandala Symbolism*, he stated, “Even the mere attempt in this direction usually has a healing effect, but only when it is done spontaneously. Nothing can be expected from an artificial repetition or deliberate imitation of such images” (p. 5).

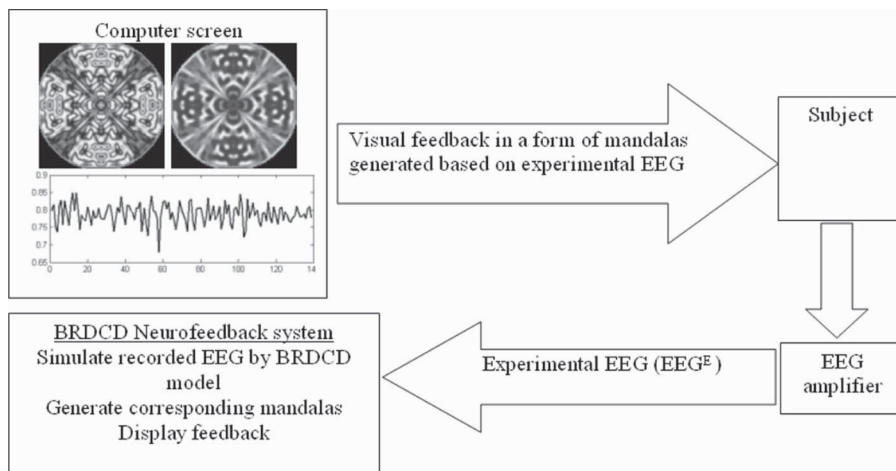
Jung wrote about a series of mandala images painted by one of his patients over a number of years (Jung, 1973). The series started with the spontaneous appearance of certain pictures in the patient’s mind. Although patient had no artistic skills or previous experience in painting, Jung encouraged her to express her fantasies in painting. He considered the appearance of such images as attempts by the subconscious to reveal its content by way of “individuation.” He tried to interpret the images but did not reveal his thoughts to the patient. As the therapy advanced, the pictures changed, reflecting changes in the patient’s mental state and at the same time aiding her progress. In our opinion, this “therapy” presents an example of a pro-neurofeedback training process.

Jung’s findings reveal the rich potential of mandalas for neurofeedback. But if we want to use them in practice, we are faced with the problem of how to replicate brain creativity processes in the form of images. Here, it

seems that the general problem lies in constructing a theoretical model of brain functioning that will combine neuronal electrical activity (as observed by EEG) with the creative patterns, such as mandalas, that emerge from this activity. Such a theoretical model should connect the internal biochemical processes taking place in the brain neurons with macrocharacteristics reflecting the collective behavior of the brain neurons responsible for brain functioning. The biochemical reactions discrete chaotic dynamics (BRDCD) model visualizes brain processes in the form of creative images, as proposed in Gontar (1997, 2000, 2003, 2004).

Here, we intend to apply the BRDCD mathematical model for fitting, online in a neurofeedback loop, the measured EEG of an individual, denoted EEG^E , to BRDCD-generated images corresponding to a theoretical time series (EEG^T). The simulated images will be directly related to the experimentally measured biological signals (EEG^E) of our test participant, which reflect the participant’s mental state. Exploiting the proposed BRDCD mathematical model that formally connects—and provides visualization of—a participant’s mental state with the BRDCD images, we can implement a neurofeedback system of visual stimuli (generated images,

FIGURE 1. Block diagram of the proposed neurofeedback method. Note. BRDCD = biochemical reactions discrete chaotic dynamics.



as shown in Figure 1). In the light of the experience of Jung, we expect that BRDCCD-based neurofeedback will provide fast and effective neurofeedback training.

BACKGROUND AND METHODOLOGY

According to BRDCCD, each neuron can be simulated as a “biochemical reactor” that has the ability to exchange information with all the other neurons connected to it (Figure 2). By “information exchange,” we mean another channel of interaction in addition to mass (via chemical reactions), charge, and energy exchange. In BRDCCD, information exchange is formally taken into consideration by establishing the dependence of the model’s parameters (rate constants) from the states of other neurons characterized by the concentrations of the chemical constituents within the neurons. The entire complex interconnected network operates according to some initial hypothesis about the mechanism of biochemical reactions in the individual neuron including information exchange between the neurons. The computations of such a mathematical model should correspond to the real distributions of the chemicals of the neuronal masses

and the evolution of these distributions in time and space.

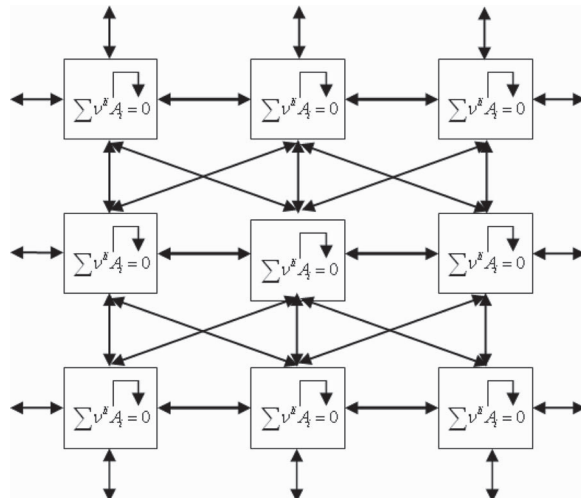
We assume that distributed chemical concentrations of neuronal networks are responsible for mental activity, including creativity. According to this basic premise, an artistic image would initially appear in the brain in the form of the distributed chemical concentrations of the neurons, and the output would then be a concrete pattern created by the individual. This pattern could be visualized by the proposed mathematical model (Gontar & Grechko, 2006b).

BRDCCD basic equations may be constructed for any mechanism involving transformations of the constituents of a system, which are expressed by a matrix of stoichiometric coefficients, and formally including into the consideration information exchange between the constituents:

$$\sum_{i=1}^N \nu^{li} A_i = 0, i = 1, 2, \dots, N, l = 1, 2, \dots, N - M \quad (1)$$

In Equation 1, as shown in Figure 2 denote information exchange between neurons. According to chemical reactions discrete chaotic dynamics, in any transfor-

FIGURE 2. Network of discrete space-distributed interconnected neurons, with each neuron representing an individual “biochemical reactor” (where A_i denotes chemical constituents and ν^{li} is a matrix of stoichiometric coefficients).

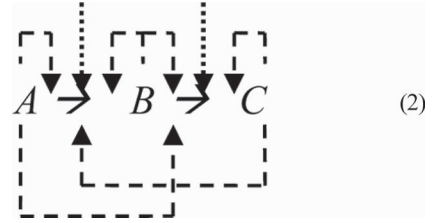


mation mechanism, a system's constituents can be represented in discrete time t_q ($q = 0, 1, 2, \dots, Q$) and discrete two-dimensional space designated by the integer coordinates $-\infty < R_p, R_s < \infty$, where p is the index denoting the rows and s is the index denoting the columns. For practical reasons, we limit our consideration to a discrete square lattice of final size $R \times R$, with coordinates

$$R_p, R_s = 1, 2, \dots, R.$$

The basic equations of BRDCD, when written for a particular mechanism of transformation of constituents and solved in discrete time and space, provide a practically unlimited source of complex signals in the form of discrete time-series that encompass chaotic and complex patterns in the form of two-dimensional images, including mandalas. These results are used in the proposed methodology for a biofeedback system.

Let us consider one of the simplest initial hypotheses about a possible mechanism of chemical transformations taking place in an individual neuron. The hypothesis describes the interaction between three chemical constituents, A , B , and C :



where the solid arrows denote the chemical transformations of the constituents, the broken-line arrows denote information exchange between the constituents inside each cell of the lattice, and the finely dotted arrows denote information exchange between the constituents in a particular cell and the constituents in the closest neighboring cells.

For this particular mechanism, a system of three nonlinear algebraic difference equations that describes the spatial-temporal dynamics of the neuronal network just presented can be derived from the basic equations of the BRDCD approach. For consistency of presentation, we repeat the description of the BRDCD mathematical model for mechanism (2) given in Gontar and Grechko (2006a, 2006b, 2007).

$$X_1^{t_q}(R_p, R_s) = \frac{b}{1 + \pi_1(X_i^{t_{q-1}}(r \otimes)) + \pi_1(X_i^{t_{q-1}}(r \otimes))\pi_2(X_i^{t_{q-1}}(r \otimes))} \quad (3)$$

$$X_2^{t_q}(R_p, R_s) = \frac{b\pi_1(X_i^{t_{q-1}}(r \otimes))}{1 + \pi_1(X_i^{t_{q-1}}(r \otimes)) + \pi_1(X_i^{t_{q-1}}(r \otimes))\pi_2(X_i^{t_{q-1}}(r \otimes))} \quad (4)$$

$$X_3^{t_q}(R_p, R_s) = \frac{b\pi_1(X_i^{t_{q-1}}(r \otimes))\pi_2(X_i^{t_{q-1}}(r \otimes))}{1 + \pi_1(X_i^{t_{q-1}}(r \otimes)) + \pi_1(X_i^{t_{q-1}}(r \otimes))\pi_2(X_i^{t_{q-1}}(r \otimes))} \quad (5)$$

where

$$\pi_1(X_i^{t_{q-1}}(r \otimes)) = k_1 \exp \left\{ - \left[\sum_{i=1}^3 \alpha_i X_i^{t_{q-1}}(R_p, R_s) + \sum_{i=1}^3 \beta_i X_i^{t_{q-1}}(r \otimes) \right] \right\} \quad (6)$$

$$\pi_2(X_i^{t_{q-1}}(r \otimes)) = k_2 \exp \left\{ - \left[\sum_{i=1}^3 \alpha_i X_i^{t_{q-1}}(R_p, R_s) + \sum_{i=1}^3 \beta_i X_i^{t_{q-1}}(r \otimes) \right] \right\} \quad (7)$$

with the initial and boundary conditions:

$$X_i^{t_0}(R_p, R_s) = \begin{cases} b_j, & i=j \\ 0, & i=M+1, M+2, \dots, N \end{cases} \quad (8)$$

$$X_i^{t_q}(R_p, R_s) = \begin{cases} X_i^{t_q}(R_p, R_s), & 1 \leq R_p, R_s \leq R \\ 0, & R_p, R_s < 1; R_p, R_s > R \end{cases} \quad \begin{array}{l} \text{(inside the lattice)} \\ \text{(outside the lattice)} \end{array} \quad (9)$$

where $X_i^{t_q}(R_p, R_s)$ is the concentration of the i th constituent that is calculated in each cell of the lattice with coordinates (R_p, R_s) and that characterizes the system's particular state at discrete time t_q ($q=1, 2, \dots, Q$); $\pi_l(t_{q-1}, r\otimes)$ is a function of the concentrations of the system's constituents $X^{t_{q-1}}(R_p, R_s)$ calculated at a previous moment of discrete time t_{q-1} and of the neighboring concentrations $X_i^{t_{q-1}}(r\otimes)$; b_j is the total concentration of the j th main constituent; k_l is the rate constant for the l th reaction; α_{li} are empirical parameters that characterize the local information exchange taking place between the constituents inside the considered cell of the lattice; and β_{li}^r are empirical parameters that characterize information exchange between the constituents in eight closest neighboring cells, including the cell under consideration ($r=1, 2, \dots, 9$), with coordinates denoted by:

$$\begin{aligned} r\otimes = & [(R_p - 1, R_s - 1), (R_p - 1, R_s), \\ & (R_p - 1, R_s + 1), (R_p, R_s - 1), \\ & (R_p, R_s), (R_p, R_s + 1), \\ & (R_p + 1, R_s - 1), \\ & (R_p + 1, R_s), (R_p + 1, R_s + 1)]. \end{aligned}$$

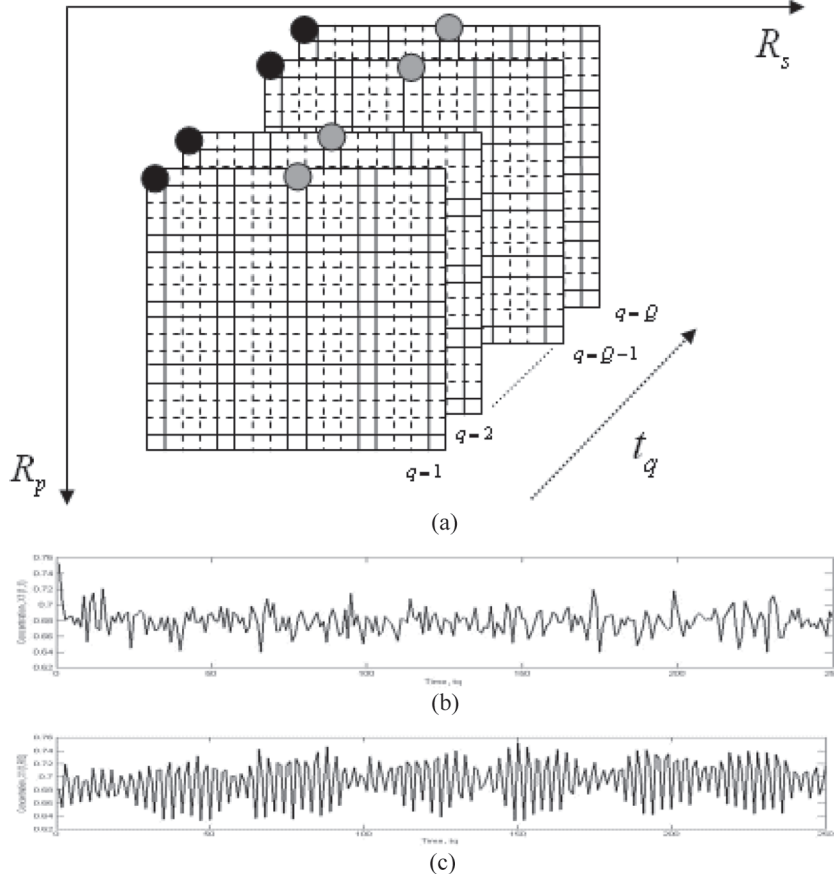
The mathematical model 3 to 5 has nine parameters ($b, k_1, k_2, \alpha_1, \alpha_2, \alpha_3, \beta_1, \beta_2, \beta_3$) that should be defined according to the type of image desired (symmetrical, nonsymmetrical, spiral, etc.). For any given set of parameters, Equations 3 to 5 generate a sequence of lattice-distributed concentrations (Figure 3) of the three chemical constituents ($X_1^{t_q}(R_p, R_s), (X_2^{t_q}(R_p, R_s)$ and

$X_3^{t_q}(R_p, R_s)$). A schematic representation of this process is shown in Figure 3. Each cell in this lattice represents the concentration of a single chemical constituent (e.g., $X_1^{t_q}(R_p, R_s)$ in an individual neuron). Therefore, if we pick, for example, the neuron in the upper left corner (marked by black circles in Figure 3a) and plot concentrations of the chosen constituent over time t_q , we obtain a discrete time-series corresponding to the evolution of the concentrations within the individual neuron (Figure 3b).

The evolution of the entire neuronal network on the considered lattice can be visualized as a sequence of colored images. For this purpose, we assign to each concentration value (Figure 4b) a particular color from a color palette (Figure 4a). In this way, equal values are visualized with the same color (as designated, e.g., with red circles in Figure 4c). Therefore, we obtain an image that represents the discrete space (lattice)-distributed concentrations of the constituent $X_1^{t_q}(R_p, R_s)$ for a given instant of time t_q .

Figure 5 presents some examples of images generated by the aforementioned mathematical model (Equations 7–9). As can be seen, these images meet the criteria for the mandalas described by Jung: they constitute circular patterns with symmetry of four crosses (“quaternity”). The mandala images presented in Figure 5 differ one from the other, and this difference in forms and colors depends on the parameters of the mathematical model. It is obvious that different sequences of images will correspond to different discrete time-series (amplitude, frequency) generated by each cell of the lattice (neurons).

FIGURE 3. (a) Schematic representation of discrete time and space, where each cell (neuron) contains chemical's concentrations that change with the discrete time t_q . (b) Example of a discrete time-series representing temporal evolution of the concentration of the chemical constituent within the individual neuron (marked by black spots). (c) Example of discrete time-series from another neuron (indicated by gray spots).



Now let us apply linear superposition (Equation 10) for these discrete time series to obtain an integrated signal representing the temporal dynamics of the whole neuronal network under consideration, where θ_i are empirically defined parameters:

$$\text{EEG}^T = \sum_{i=1,2,\dots,R \times R} \theta_i X_i^{t_q} (r \otimes) \quad (10)$$

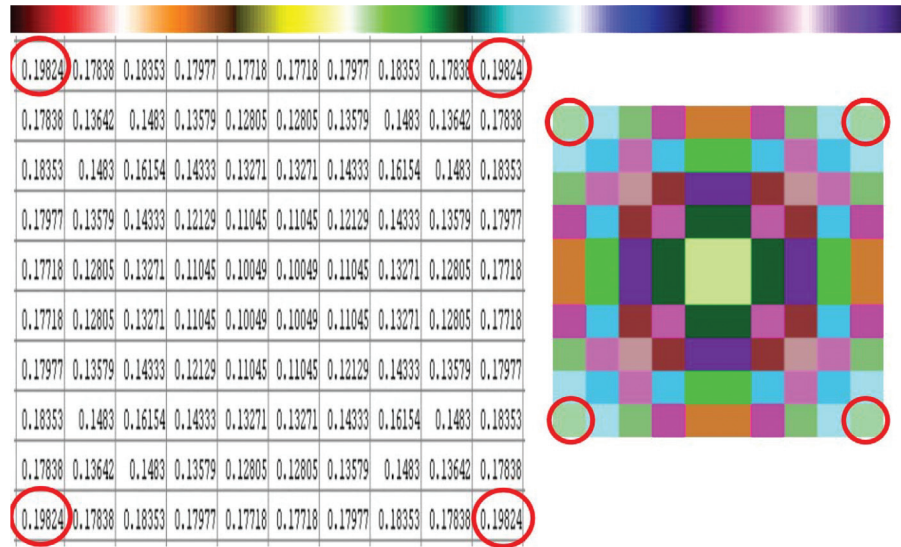
We call this integrated signal, which reflects the temporal dynamics of the whole lattice-distributed neuronal network under consideration, a “simulated EEG signal” or EEG^T . Figure 6a and b presents two examples of integrated EEG^T signal obtained for $\theta_i = 0.5, \forall i$ and for two different sets of

parameters ($b, k_1, k_2, \alpha_1, \alpha_2, \alpha_3, \beta_1, \beta_2, \beta_3$), Equations 3 to 5.

To combine signals from two (or more) local neuronal networks, we propose to apply superposition 10 of already-integrated signals resulting from different neuronal networks. This procedure will constitute a more realistic approach to the brain functioning, where different parts of the brain (presented by local neuronal networks) operate in parallel to contribute to the measured integrated EEG^E and should therefore be taken into account. Figure 6c presents an example of an integrated EEG^T signal for two different neuronal networks.

To apply the aforementioned methodology, one can establish a correlation between EEG^T , that is, an EEG simulated by a

FIGURE 4. Encoding of the calculated concentration of one of the neuron's constituents by means of a color palette (a). Equal values shown in (b) are encoded with the same color, as for example, values marked by red circles (c).



BRDCD time-series, and an experimentally measured EEG^E. It can be shown that direct comparison of the simulated and measured time series in terms of their synchronized

amplitudes by using the least-squares method is computationally ineffective. Therefore, we propose to fit the experimental data to our model in the frequency domain.

FIGURE 5. Examples of mandala images generated by biochemical reactions discrete chaotic dynamics BRDCD.

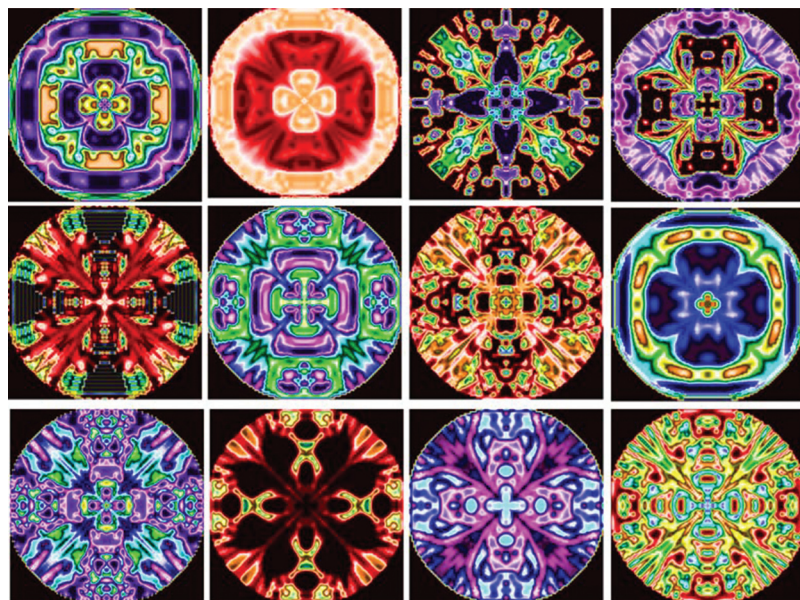
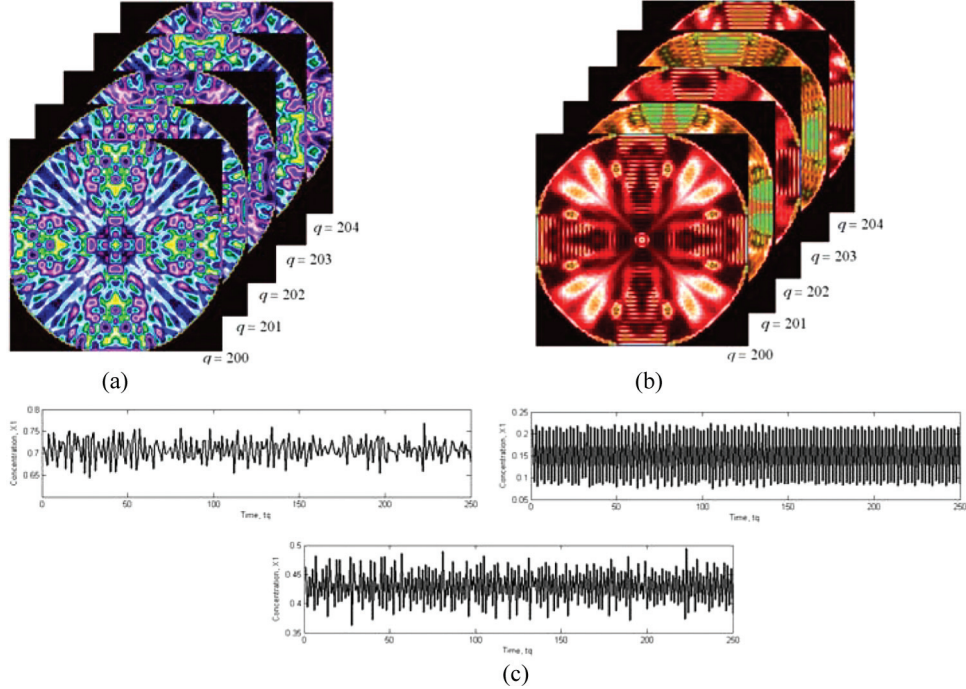


FIGURE 6. (a, b) Examples of simulated EEG^T signals for two different series of mandala images. (c) Example of combined signal coming from two different groups of neurons: combination of the integrated signals presented in Figure 6a and 6b.



The fitting is achieved by varying the nine parameters of the model (Equations 3–5) so as to minimize the least-squares difference between the spectrum of the experimental EEG^E and that of the theoretical EEG^T.

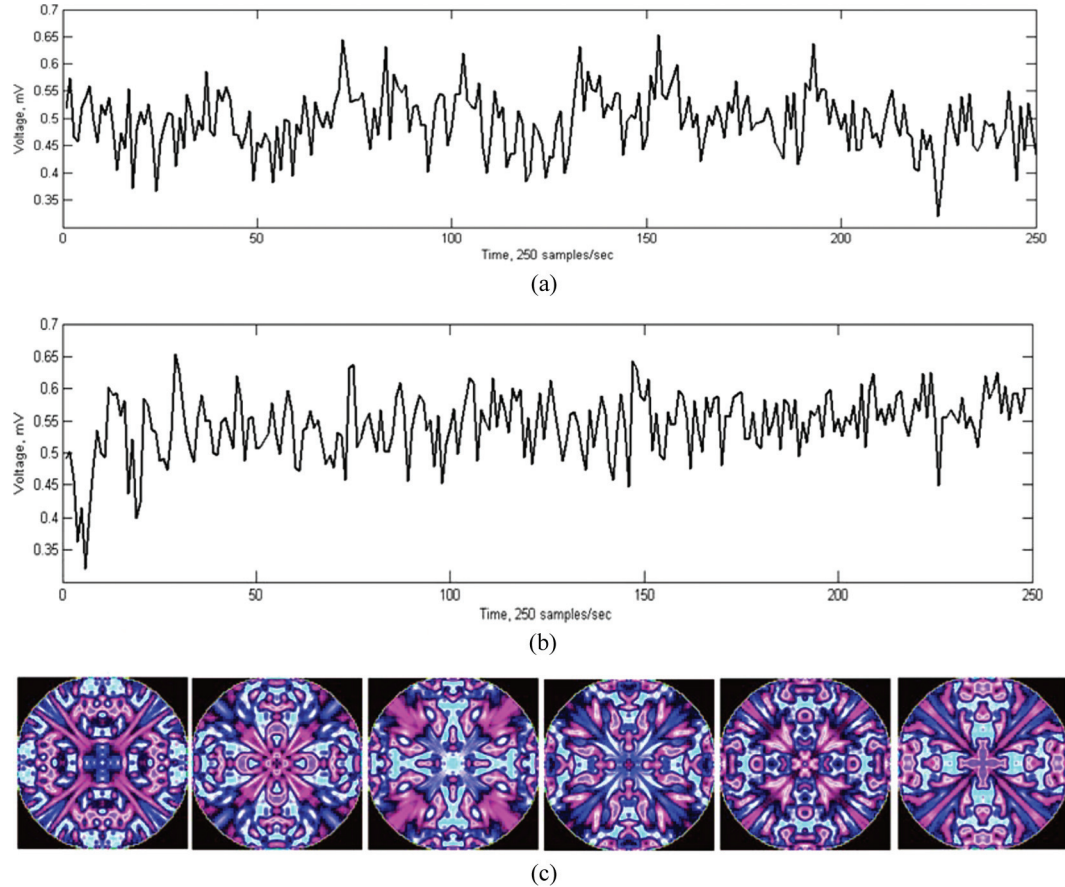
RESULTS

In this section, we present experimental verification of our theoretical approach. We applied the aforementioned methodology to EEG^E signals with the aim of generating a corresponding series of images. For recording the EEG^E, we used a custom-built EEG amplifier with four channels and a sampling rate of 250 samples per second. Disposable golden electrodes were used in the experiment. EEG^E signals were obtained using single channel assessment (referential montage with reference to ear lobes). The recording was accomplished with a gain of 5,000, providing us with a full-scale 1-mV peak-to-peak. The filters were set at low pass

(LP) 125 Hz (24 db/octave) and high pass (HP) 0.16 Hz (12 db/octave). We applied neither digital filtering nor artifacts removal. Our participant was healthy 29-year-old man with no known medical problems.

Figure 7 (upper panel) shows a 1-s segment of a raw EEG^E recorded over Pz with the participant's eyes open (upper part). The central panel of the figure shows the integrated time-series generated by the BRDCD mathematical model, which represents the temporal dynamics of 10,000 neurons (250 iterations corresponding to 250 samples of the 1-s EEG^E segment). The lower panel of Figure 7 presents a representative sample of 6 of the 250 mandala images corresponding to the simulated signal. To analyze correspondence of the EEG^T and EEG^E signals we compared these two segments by computing their bandwidth spectra (Figure 8). Here we can clearly see the qualitative correspondence of these two signals within the 1–40 Hz frequency domain (we have omitted high frequencies on a plot [Figures 8 and 10],

FIGURE 7. (a) One-s (250 samples) segment of an experimental raw EEG^E recorded over Pz with eyes open. (b) One-s (250 samples) segment of an EEG simulated by biochemical reactions discrete chaotic dynamics. (c) Examples of 6 ($q=1, 50, 100, 150, 200, 250$) of 250 mandala images corresponding to the simulated EEG^T.



but they were included into consideration for EEG spectral analyses).

Figure 9a shows a 1-s segment of a raw EEG^E recorded over Cz with the participant's eyes closed. Figure 9b shows the integrated time-series generated by the BRDCD mathematical model, which represents the temporal dynamics of 10,000 neurons (250 iterations corresponding to 250 samples of the 1-s EEG^E segment). Figure 9c presents six mandala images chosen arbitrarily and corresponding to six t_q values ($q=1, 50, 100, 150, 200, 250$) of the signal in Figure 9b. Again, the qualitative resemblance between EEG^E and EEG^T can be seen and was confirmed by the corresponding spectra (Figure 10).

CONCLUSIONS

The proposed method for neurofeedback provides a direct connection between experimental EEG^E signals and the states of spatially distributed neuronal networks in the form of colored symmetrical images—mandalas. We propose to use the EEG-related mandalas as visual stimuli in a neurofeedback training process. In view of the belief of Jung—that mandala images, being generated involuntarily, may have a therapeutic effect on a person's mental health—we predict that stimuli of this kind could provide fast and effective training. The mandalas generated involuntarily according to the mental state of our test

FIGURE 8. (a) Bandwidths of the experimental EEG^E shown in (a). (b) Bandwidths of the EEG^T simulated by biochemical reactions discrete chaotic dynamics, shown in (b).

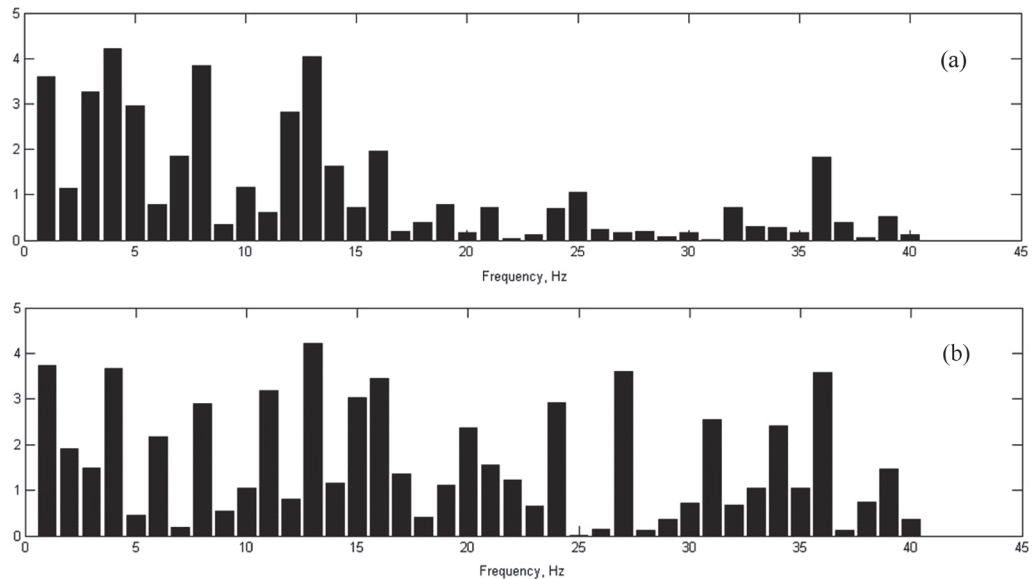


FIGURE 9. (a) One-s (250 samples) segment of the raw EEG^E recorded over Cz with the participant's eyes closed. (b) One-s (250 samples) segment of an EEG^T simulated by biochemical reactions discrete chaotic dynamics. (c) Example of 6 ($q=1, 50, 100, 150, 200, 250$) of 250 mandala images corresponding to the simulated EEG^T.

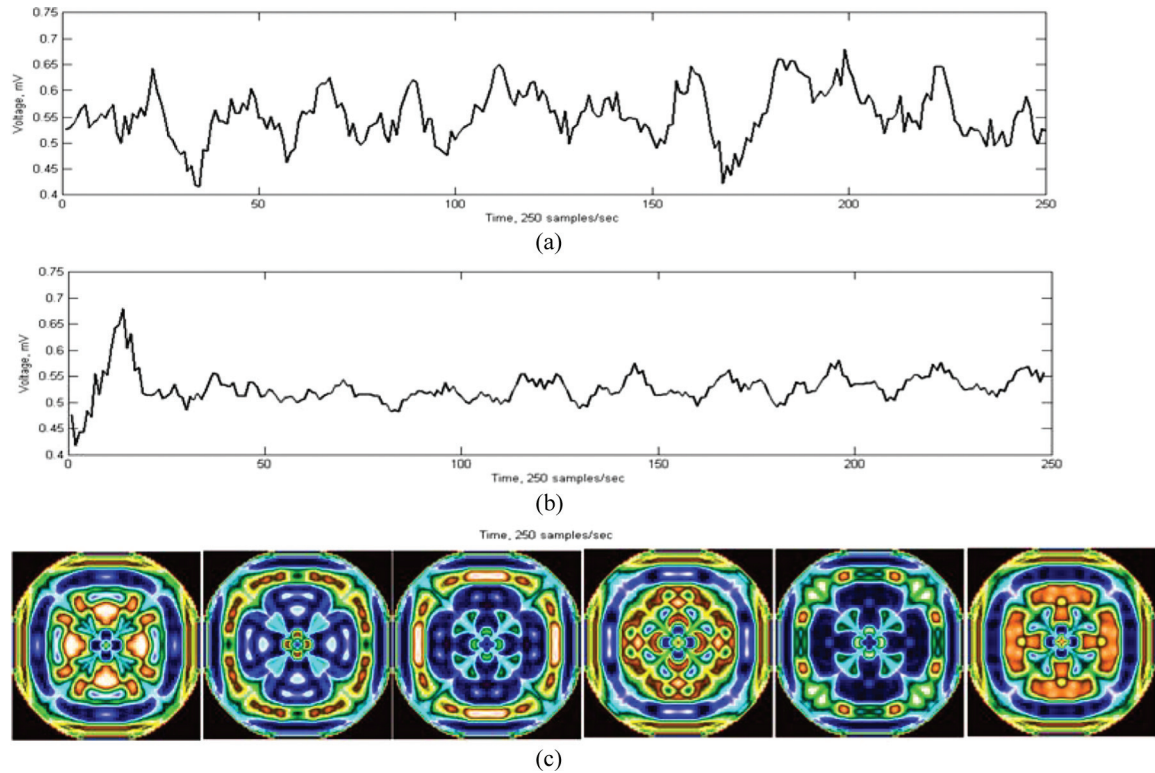
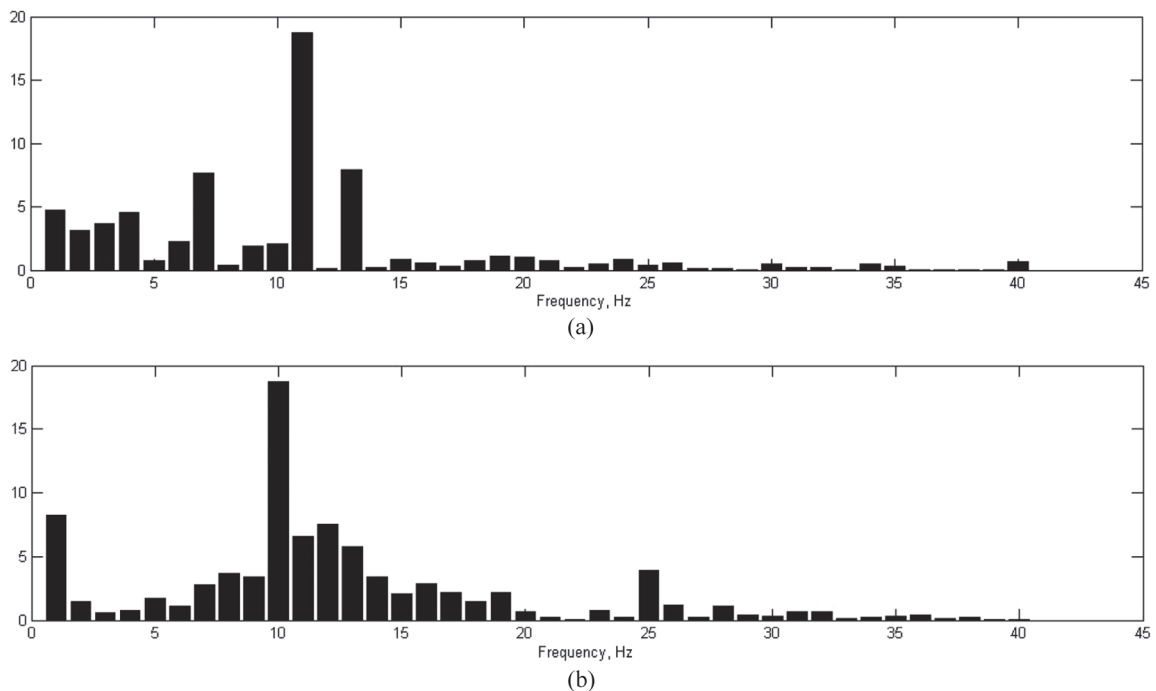


FIGURE 10. (a) Bandwidths of experimental EEG^E. (b) Bandwidths of EEG^T simulated by biochemical reactions discrete chaotic dynamics.



participant—as presented by his EEG—should fit the requirements of Jung. Experimental verification of the proposed principles for constructing a neurofeedback system demonstrates sufficient correspondence between real EEG^E signals and those modeled by BRDCCD. EEG^E-related colored symmetrical images generated by the BRDCCD mathematical model demonstrated presence of the basic features of mandalas described by Jung, that is, circular images containing patterns in multiples of four in the form of a cross, a star, a square, and so on.

REFERENCES

- Gontar, V. (1997). Theoretical foundation for the discrete chaotic dynamics of physicochemical systems: Chaos, self-organization, time and space in complex systems. *Discrete Dynamics in Nature and Society*, 1, 31–44.
- Gontar, V. (2000). Theoretical foundation of Jung's "Mandala Symbolism" based on discrete chaotic dynamics of interacting neurons. *Discrete Dynamics in Nature and Society*, 5, 19–28.
- Gontar, V. (2003). Artificial brain systems based on discrete chaotic dynamics of interacting intellectual agents. In *Proceedings of the International Conference on Computer Science and Its Applications* (pp. 1–3). San Diego, CA: National University US Education Service.
- Gontar, V. (2004). The dynamics of living and thinking systems, biological networks and the laws of physics. *Discrete Dynamics in Nature and Society*, 8, 101–111.
- Gontar, V. & Grechko, O. (2006a). Fractal sets generated by chemical reactions discrete chaotic dynamics. *Chaos, Solitons and Fractals*, 32, 496–502.
- Gontar, V. & Grechko, O. (2006b). Generation of symmetrical colored images via solution of the inverse problem of chemical reactions discrete chaotic dynamics. *International Journal of Bifurcation and Chaos*, 16, 1–16.
- Gontar, V. & Grechko, O. (2007). Some aspects of mathematical imaging using chemical reactions discrete chaotic dynamics. *Fractals*, 15, 315–322.
- Jung, C. G. (1973). *Mandala symbolism*. Princeton, NJ: Princeton University Press.
- Thompson, M. & Thompson, L. (2003). *The neurofeedback book*. Wheat Ridge, CO: The Association for Applied Psychophysiology and Biofeedback.

Copyright of Journal of Neurotherapy is the property of Haworth Press and its content may not be copied or emailed to multiple sites or posted to a listserv without the copyright holder's express written permission. However, users may print, download, or email articles for individual use.